Defense Technical Information Center Compilation Part Notice

ADP011839

TITLE: Liquid Crystal Aberration Compensation Devices

DISTRIBUTION: Approved for public release, distribution unlimited

This paper is part of the following report:

TITLE: Optical Storage and Optical Information Held in Taipei, Taiwan on 26-27 July 2000

To order the complete compilation report, use: ADA399082

The following component part numbers comprise the compilation report:
ADP011833 thru ADP011864

Invited Paper

Liquid crystal aberration compensation devices

Sjoerd Stallinga[a], Joris Vrehen[b], Jeroen Wals[b], Henk Stapert[a], and Emile Verstegen[a]

[a]Philips Research Laboratories, Professor Holstlaan 4, 5656 AA Eindhoven, The Netherlands
[b]Philips Optical Storage, Glaslaan 1, 5600 JB Eindhoven, The Netherlands

ABSTRACT

The application of aberration compensation devices can support the trend to higher information densities in optical data storage. The information content of a disc may be increased while maintaining acceptable tolerance levels. For example, disc tilt dependence may require coma compensation, whereas double layer formats require spherical aberration compensation. Liquid crystals (LCs) can be successfully applied in such devices. The design of two practical implementations is discussed; a coma compensating LC-cell with special electrode-design for optimized tolerances w.r.t. decentering, and a lens made of photopolymerizable LC, which can be used to compensate for spherical aberration.

Keywords: aberration compensation, coma, spherical aberration, disc tilt, cover layer thickness, dual layer, liquid crystal, birefringent lens

1. INTRODUCTION

In the field of optical disc storage there is a continuous push to higher information densities. This is achieved by using a small wavelength λ and a high numerical aperture NA, as the spot size is roughly λ/NA. Table 1 shows that the NA increases from 0.45 for CD (Compact Disc) to 0.60 for DVD (Digital Versatile Disc), and even 0.85 for DVR (Digital Video Recorder),[1] while the wavelength decreases. The increase in NA and the decrease in λ lead to an increased sensitivity to aberrations. A measure for this sensitivity is the number $(d/\lambda)\mathrm{NA}^k$, with d the cover layer thickness and $k = 2$ for defocus and astigmatism, $k = 3$ for coma, and $k = 4$ for spherical aberration. Clearly, a large NA and a small λ are disavantageous from the point of view of aberrations. Important causes of aberrations are disc tilt, which gives rise to coma, and cover layer thickness variations, which give rise to spherical aberration. Table 1 shows the numbers $(d/\lambda)\mathrm{NA}^k$ for CD, DVD, and DVR. As indicated by these numbers DVD has a coma problem, and DVD and DVR a spherical aberration problem. It turns out that the problem is slightly worse for DVR, because of higher order aberrations (with larger powers k).

Table 1. Aberration sensitivity of CD, DVD, and DVR.

format	NA	λ	d	$(d/\lambda)\mathrm{NA}^2$	$(d/\lambda)\mathrm{NA}^3$	$(d/\lambda)\mathrm{NA}^4$
CD	0.45	780 nm	1.2 mm	0.31×10^3	0.14×10^3	0.06×10^3
DVD	0.60	650 nm	0.6 mm	0.33×10^3	0.20×10^3	0.12×10^3
DVR	0.85	400 nm	0.1 mm	0.18×10^3	0.15×10^3	0.13×10^3

Adaptive compensation of aberrations solves the increased aberration sensitivity in high NA optical storage formats. The widened design margins may be quite advantageous. An important type of aberration compensator uses liquid crystals (LCs). These birefingent liquids can be used to make an electrically controlable phase plate. This phase plate consists of an LC-cell with segmented (and transparant) electrodes. The voltage on each electrode translates into an angle ψ between the substrate normal and the director (the uniaxial symmetry axis of the liquid crystal). The extraordinary polarization mode has a refractive index depending on ψ:

$$n_{\mathrm{eff}} = \frac{n_{\mathrm{o}} n_{\mathrm{e}}}{\sqrt{n_{\mathrm{o}}^2 \sin^2\psi + n_{\mathrm{e}}^2 \cos^2\psi}}, \tag{1}$$

Correspondence to Sjoerd Stallinga, E-mail: sjoerd.stallinga@philips.com

In *Optical Storage and Optical Information Processing*, Han-Ping D. Shieh, Tom D. Milster, Editors, Proceedings of SPIE Vol. 4081 (2000) • 0277-786X/00/$15.00

with n_o and n_e the ordinary and extraordinary refractive index, respectively. It follows that the refractive index for each electrode segment (and thereby the optical path length) can be varied between n_o and n_e by an electric signal. A suitable aberration compensator can be made by a proper choice of the shape and number of segments. An alternative method of making an LC aberration compensator uses a single non-segmented electrode and a non-flat substrate, leading to a non-constant LC layer thickness. The tilt angle ψ does not depend on the layer thickness, meaning that the single voltage gives rise to a uniform tilt angle ψ and thus to a uniform refractive index. The surface profile then reflects the aberration that is compensated, and the applied voltage is a measure for the amount of the compensation. For instance, when the thickness is $d_0 + d_1\rho^4$, with ρ the polar pupil coordinate, the cell can be used to compensate for spherical aberration.

Two examples of LC aberration compensators are discussed in this paper, a disc tilt compensator of the segmented electrode type for DVD, and a cover layer variation compensator of the surface profile type for DVR.

2. DISC TILT COMPENSATION

2.1. The Zernike Cell

Disc tilt causes a spot that is aberrated by coma. The compensating LC-cell must therefore add coma of the opposite sign. Coma has a phase profile in the pupil plane proportional to the Zernike polynomial:

$$Z_{31}(x,y) \;=\; \left[3(x^2+y^2)-2\right]x \;=\; \left(3\rho^3-2\rho\right)\cos\theta\,, \tag{2}$$

where x and y are the Cartesian pupil coordinates, and ρ and θ the polar pupil coordinates. Appropriate and simple electrode segments for the compensating LC-cell are given by the recipe:

- The pupil region for which $Z_{31}(x,y) > a$ is a segment, with voltage V_+.
- The pupil region for which $a \geq Z_{31}(x,y) \geq -a$ is a segment, with voltage V_0.
- The pupil region for which $-a > Z_{31}(x,y)$ is a segment, with voltage V_-.

The voltages satisfy $V_\pm = V_0 \pm \Delta$. If the voltage modulation Δ is sufficiently small, the phase modulation is linear in Δ. Note that the applied voltages are in fact AC-voltages, so V_0, V_+, and V_- are really the *amplitudes* of the voltage signals. Fig. 1, left figure, shows such a Zernike cell for $a = 0.21$. LC-cells of this type have already been proposed in the literature.[2]

The improvement that can be obtained can be estimated as follows. Suppose that the original comatic aberration due to disc tilt is $A_{31}Z_{31}(x,y,)$, where A_{31} is a constant proportional to the disc tilt α. The RMS wavefront aberration is then given by:

$$\mathrm{RMS}_0^2 \;=\; A_{31}^2 \int \mathrm{d}x\mathrm{d}y\; Z_{31}(x,y)^2\,, \tag{3}$$

where the integration range extends over the pupil (the unit circle), and where a multiplicative constant is ignored. The phase profile added by the LC-cell is $\Phi_{\mathrm{LC}}(x,y) = B\Gamma_{\mathrm{LC}}(x,y)$, where $\Gamma_{\mathrm{LC}}(x,y)$ is the phase profile with unit modulation and B is a constant proportional to the voltage modulation Δ. The RMS wavefront aberration is now:

$$\mathrm{RMS}^2 \;=\; \int \mathrm{d}x\mathrm{d}y\; \left[A_{31}Z_{31}(x,y) + B\Gamma_{\mathrm{LC}}(x,y)\right]^2\,, \tag{4}$$

and has a minimum when the constant B satisfies:

$$B \;=\; -A_{31}\frac{\int \mathrm{d}x\mathrm{d}y\; Z_{31}(x,y)\Gamma_{\mathrm{LC}}(x,y)}{\int \mathrm{d}x\mathrm{d}y\; \Gamma_{\mathrm{LC}}(x,y)^2}\,. \tag{5}$$

It follows that B is linear in A_{31}. As a consequence, the voltage modulation Δ is linear in the disc tilt α. This minimum RMS wavefront aberration can be obtained from the relative decrease in the square of the RMS wavefront aberration:

$$\frac{\mathrm{RMS}_0^2 - \mathrm{RMS}^2}{\mathrm{RMS}_0^2} \;=\; \frac{\left[\int \mathrm{d}x\mathrm{d}y\; Z_{31}(x,y)\Gamma_{\mathrm{LC}}(x,y)\right]^2}{\int \mathrm{d}x\mathrm{d}y\; Z_{31}(x,y)^2 \quad \int \mathrm{d}x\mathrm{d}y\; \Gamma_{\mathrm{LC}}(x,y)^2}\,, \tag{6}$$

This quantity is a measure for the match between the Zernike coma and the LC phase profile. The parameter a is determined from the requirement that this measure is maximum. It turns out that the maximum is 0.85 and is obtained for $a = 0.21$. The remaining RMS is then $\sqrt{1-0.85} = 0.39$ of the original RMS_0 due to disc tilt. This remaining RMS consists of higher order aberrations. Maximum improvement of the disc tilt margin is obtained when disc tilt is the only error. In that case the RMS is proportional to the tilt angle α. The spot on the disc is then still diffraction limited for a tilt angle that is 1/0.39=2.58 higher than without the LC-compensator. The improvement in tilt margin is 158%. In practice, there are other errors in the readout of the disc, and the improvement in tilt margin is not so large.

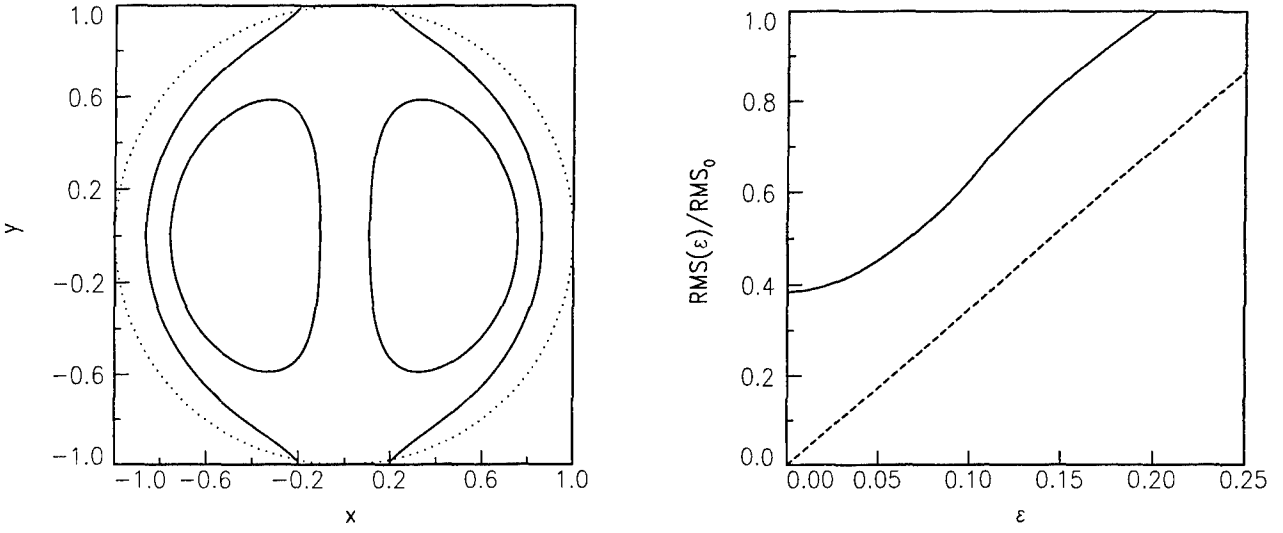

Figure 1. Left: Shape of the segmented electrode structure of the Zernike cell. Leads to the two inner segments pass through the central segment, but are not drawn in this figure. The pupil rim (for zero decentering) is indicated with a dotted line. Right: Ratio of the RMS wavefront aberration to the original comatic RMS wavefront aberration as a function of the decenter ε (full line), and the astigmatic approximation to this ratio (dashed line).

2.2. Decentering of the Objective Lens

The Zernike cell no longer works properly when the objective lens is decentered w.r.t. the fixed light path. The LC cell now generates a phase profile $B\Gamma_{\mathrm{LC}}(x-\varepsilon, y)$ instead of the original $B\Gamma_{\mathrm{LC}}(x, y)$. Here, ε is the objective lens displacement in units of the pupil radius. The RMS wavefront aberration as a function of ε can be obtained from:

$$\frac{\mathrm{RMS}_0^2 - \mathrm{RMS}(\varepsilon)^2}{\mathrm{RMS}_0^2} = \frac{\mathrm{RMS}_0^2 - \mathrm{RMS}(0)^2}{\mathrm{RMS}_0^2} \left\{ 2\frac{\int \mathrm{d}x\mathrm{d}y\ Z_{31}(x,y)\Gamma_{\mathrm{LC}}(x-\varepsilon,y)}{\int \mathrm{d}x\mathrm{d}y\ Z_{31}(x,y)\Gamma_{\mathrm{LC}}(x,y)} - \frac{\int \mathrm{d}x\mathrm{d}y\ \Gamma_{\mathrm{LC}}(x-\varepsilon,y)^2}{\int \mathrm{d}x\mathrm{d}y\ \Gamma_{\mathrm{LC}}(x,y)^2} \right\}, \quad (7)$$

where RMS(0) follows from (6). Fig. 1, right figure, shows the ratio of RMS(ε) to the original comatic RMS_0 as a function of ε (full line). There is no net improvement when ε is larger than 0.20. For the fast seek feature in disc readout (a quick scan of the content of the tracks that are a few tracks ahead) it is necessary to have a margin of approximately 0.20. Consequently, the decentering margin and the tilt margin are incompatible.

The largest fraction of the aberrations generated by the decentering consists of astigmatism, as the phase profile of the LC-cell closely resembles a comatic phase profile. This can be seen using:

$$Z_{31}(x-\varepsilon, y) = \left[3(x^2+y^2)-2\right]x - 3\varepsilon\left[x^2-y^2\right] - 3\varepsilon\left[2x^2+2y^2-1\right] + 9\varepsilon^2 x - 3\varepsilon(1+\varepsilon^2). \quad (8)$$

This equation implies that a decentered coma profile contains an additional amount of astigmatism (second term) proportional to the decentering ε. The remaining terms are defocus, wavefront tilt, and piston, which are not

important. The amount of astigmatism that is generated is $A_{22} = 3\varepsilon A_{31}$, leading to a relative increase in the square of the RMS wavefront aberration:

$$\frac{\Delta \mathrm{RMS}^2}{\mathrm{RMS}_0^2} = \frac{|A_{22}|^2/6}{|A_{31}|^2/8} = 12\varepsilon^2 . \tag{9}$$

The astigmatic approximation of the numerically calculated curve in Fig. 1, right figure, is the line $\sqrt{12}\,\varepsilon$ (dashed line). Clearly, the slope of the curve agrees well with the numerical result. The difference between the two curves is nearly constant and is due to the higher order aberrations.

2.3. Solutions of the Decentering Problem

We have identified a number of different solutions to the decentering problem. The easiest one is fixing the LC-cell to the actuator. In that case there is simply no decentering of the objective lens w.r.t. the LC-cell. The disadvantage of this solution is that the weight of the actuator is increased substantially, and has therefore an adverse effect on the mechanical bandwidth.

A second solution is balancing of the coma that is compensated and the additional aberrations generated by decentering by making the coefficient B dependent on ε, instead of the fixed value given by (5). Minimum RMS is obtained when:

$$B(\varepsilon) = -A_{31}\frac{\int \mathrm{d}x\mathrm{d}y\; Z_{31}(x,y)\Gamma_{\mathrm{LC}}(x-\varepsilon,y)}{\int \mathrm{d}x\mathrm{d}y\; \Gamma_{\mathrm{LC}}(x-\varepsilon,y)^2} . \tag{10}$$

The remaining RMS is now given by a formula similar to (6):

$$\frac{\mathrm{RMS}_0^2 - \mathrm{RMS}(\varepsilon)^2}{\mathrm{RMS}_0^2} = \frac{\left[\int \mathrm{d}x\mathrm{d}y\; Z_{31}(x,y)\Gamma_{\mathrm{LC}}(x-\varepsilon,y)\right]^2}{\int \mathrm{d}x\mathrm{d}y\; Z_{31}(x,y)^2 \quad \int \mathrm{d}x\mathrm{d}y\; \Gamma_{\mathrm{LC}}(x-\varepsilon,y)^2} . \tag{11}$$

Fig. 2 (left picture) shows the balanced ratio $\mathrm{RMS}(\varepsilon)/\mathrm{RMS}_0$ (full line), which clearly improves the unbalanced ratio (dotted line). The LC phase modulation $B(\varepsilon)$ relative to the original coefficient $B(0)$ is shown in the right picture of Fig. 2 (full line).

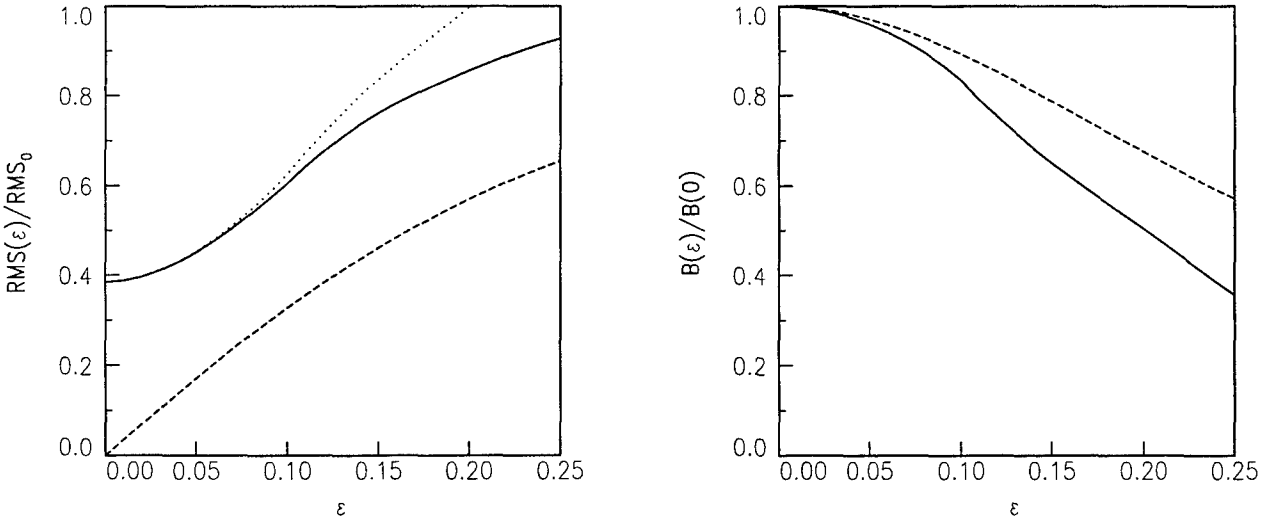

Figure 2. Left: Ratio of the balanced RMS wavefront aberration to the original comatic RMS wavefront aberration as a function of the decenter ε (full line), the astigmatic approximation to this ratio (dashed line), and the unbalanced ratio of the RMS wavefront aberration to the original comatic RMS wavefront aberration (dotted line). Right: Ratio of the LC phase modulation with balancing to the original Lc phase modulation (full line), and the astigmatic approximation (dashed line).

The balancing procedure can also be treated analytically with an approximation similar to the one described in the previous subsection. In this approximation the coma is balanced by the astigmatism that is generated. This means that only a fraction η of the coma caused by disc tilt is compensated, where η varies with the decentering ε. The remaining non-compensated coma is now $(1-\eta)A_{31}$, whereas the generated astigmatism is $A_{22} = 3\varepsilon\eta A_{31}$. This gives rise to an RMS^2 value:

$$\frac{\mathrm{RMS}^2}{\mathrm{RMS}_0^2} = (1-\eta)^2 + 12\varepsilon^2\eta^2 \,. \tag{12}$$

The minimum value is obtained when:

$$\eta = \frac{1}{1+12\varepsilon^2} \,, \tag{13}$$

and is equal to:

$$\frac{\mathrm{RMS}^2}{\mathrm{RMS}_0^2} = \frac{12\varepsilon^2}{1+12\varepsilon^2} \,. \tag{14}$$

Fig. 2 shows this minimum value (dashed line, left figure). Again, the slope of the curve agrees well with the numerical result, the nearly constant difference between the two curves being due to higher order aberrations. The LC phase modulation B is also shown in Fig. 2 (dashed line, right figure). Here, the agreement is only qualitative.

A third solution is having a second electrode structure on the opposite side of the LC-layer. On side 1 the segments are defined as:

- The pupil region for which $Z_{31}(x+\varepsilon_0, y) > a$ is one segment, with voltage $V_1 - \Delta_1$.
- The pupil region for which $a \geq Z_{31}(x+\varepsilon_0, y) \geq -a$ is one segment, with voltage V_1.
- The pupil region for which $-a > Z_{31}(x+\varepsilon_0, y)$ is one segment, with voltage $V_1 + \Delta_1$,

and on side 2:

- The pupil region for which $Z_{31}(x-\varepsilon_0, y) > a$ is one segment, with voltage $V_2 - \Delta_2$.
- The pupil region for which $a \geq Z_{31}(x-\varepsilon_0, y) \geq -a$ is one segment, with voltage V_2.
- The pupil region for which $-a > Z_{31}(x-\varepsilon_0, y)$ is one segment, with voltage $V_2 + \Delta_2$.

It follows that the electrodes on side 1 are displaced over a distance $-\varepsilon_0$ in the x direction, whereas the electrodes on side 2 are displaced over a distance $+\varepsilon_0$. This structure is schematically drawn in Fig. 3 (left figure). The voltages V_1, V_2, Δ_1 and Δ_2 are chosen such that:

$$V_1 - V_2 = V_0 \,, \tag{15}$$

$$\Delta_1 = \frac{\varepsilon_0 - \varepsilon}{2\varepsilon_0}\Delta \,, \tag{16}$$

$$\Delta_2 = \frac{\varepsilon_0 + \varepsilon}{2\varepsilon_0}\Delta \,, \tag{17}$$

When all the electric signals are in phase the amplitude at position (x, y) is the difference in the amplitude of the signals on the two sides of the LC. Consequently, the phase profile that is generated is a weighted sum of the two displaced coma profiles. For instance, if the decentering $\varepsilon = \varepsilon_0$, then $\Delta_1 = 0$ and all electrodes on side 1 have voltage V_1. On side 2, the modulation $\Delta_2 = \Delta$. This means that the original Zernike phase profile is recovered, but displaced over a distance ε, exactly what is required to compensate for the decentering of the objective lens. If $\varepsilon = -\varepsilon_0$ the roles of sides 1 and 2 are interchanged, and for other values of ε the phase profile is an interpolation between these two cases. By choosing ε_0 between 0 and the maximum objective displacement a good compensation for disc tilt can be achieved for all values of the decentering of the objective lens. Fig. 3, right figure, shows the ratio $\mathrm{RMS}(\varepsilon)/\mathrm{RMS}_0$ for $\varepsilon_0 = 0.15$. This ratio is in the range 0.40-0.45 for virtually the whole range of ε values. Finally, it is mentioned that it is also possible to have both electrode structures on the same side of the LC-cell. However, the increased number of electrodes requires additional leads to the inner segments. These additional leads pass through the other segments, thereby disturbing the phase profile.

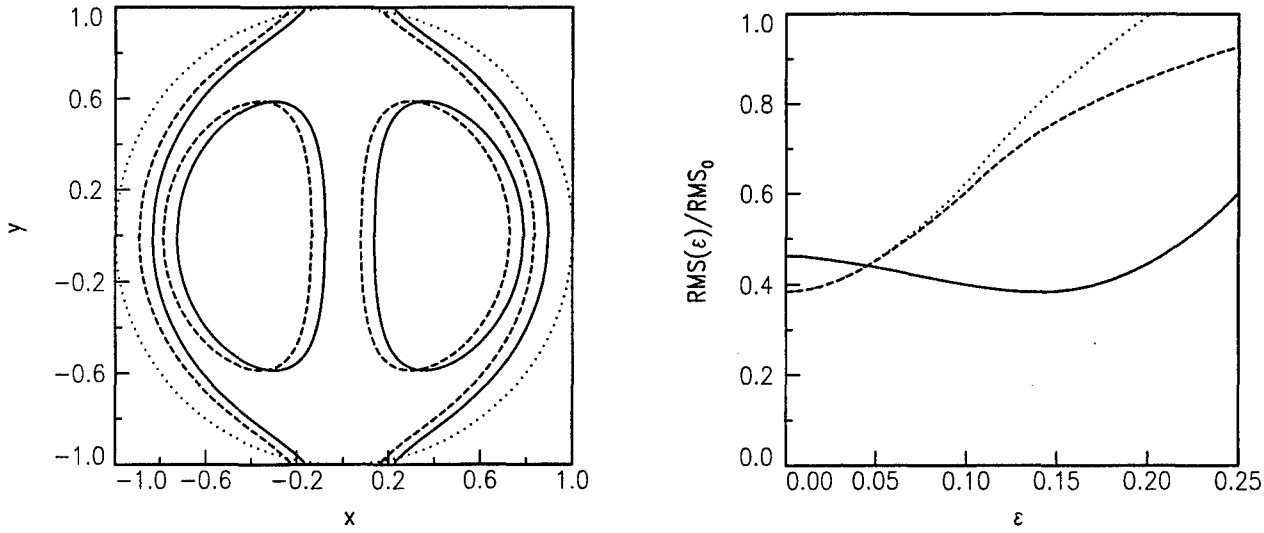

Figure 3. Left: Mutually displaced electrode segments on both sides of the doubled Zernike cell. The full lines refer to the segments on one side, the dashed lines to the segments on the other side. The pupil rim (for zero decentering) is indicated by the dotted line. Right: The ratio $\mathrm{RMS}(\varepsilon)/\mathrm{RMS}_0$ for the doubled Zernike cell with $\varepsilon_0 = 0.15$ (full line), the balanced single Zernike cell (dashed line) and the unbalanced single Zernike cell (dotted line).

2.4. The Seidel Cell

The disc tilt compensation with Zernike cells only reduces the RMS to around 40% of the original RMS because of the higher order aberrations. These aberrations are introduced by the large discontinuities in the phase profile at the edges of the electrode segments. This problem can be eliminated by increasing the number of electrode segments. However, not all segments are connected to the pupil rim, meaning that a large number of leads passing through other segments must be introduced in the design. In addition, a large number of leads from the driver IC to the LC-cell is required, which is highly unfavourable. These problems may be overcome with two changes in the design. First, we may take the Seidel coma $W_{31} = (x^2 + y^2)x$ as the basis of our compensator instead of the Zernike coma $Z_{31} = \left[3(x^2 + y^2) - 2\right] x$. The difference is a tilt term, meaning that the field of the objective lens is used. However, this effect can be neglected. For a Seidel cell the electrode segments are bent strips with varying width that are all connected to the pupil rim. Suppose the strips are numbered by an index taking values $-N, -N+1, \ldots, 0, 1, \ldots, N$. Then there are $2N+1$ strips. The strip with index j occupies the pupil region consisting of points (x, y) that satisfy:

$$\frac{2j-1}{2N+1} < W_{31}(x,y) < \frac{2j+1}{2N+1}. \tag{18}$$

Fig. 4 shows an example of such a cell with $N = 8$. The second problem is solved by making a resistor bench in the transparant conductor. The individual resistors are U-turns connecting strip j with strip $j+1$. If a voltage is applied to only a limited number of strips than the voltage on the intermediate strips is found by linear interpolation between the voltages on the nearest strips with outside leads. For instance, if strips $-N$, 0, and N have these outside leads, with voltages $V_+ = V_0 + \Delta$, V_0, and $V_- = V_0 - \Delta$, respectively, then the voltage on strip j is:

$$V_j = V_0 - \frac{j}{N}\Delta. \tag{19}$$

The match between the LC phase profile and the Seidel coma can be calculated using an expression similar to (6). It turns out that the residual RMS wavefront aberration is smaller than 10% of the original Seidel coma if $N \geq 8$. Fig. 4 (right figure) shows the decentering performance of such a Seidel cell (dotted line). The decentering problem is reduced compared to the Zernike case, but is not eliminated alltogether. A further reduction can be obtained by balancing (dashed line) or by breaking the symmetry of the applied voltages, i.e. by choosing V_+ and V_-

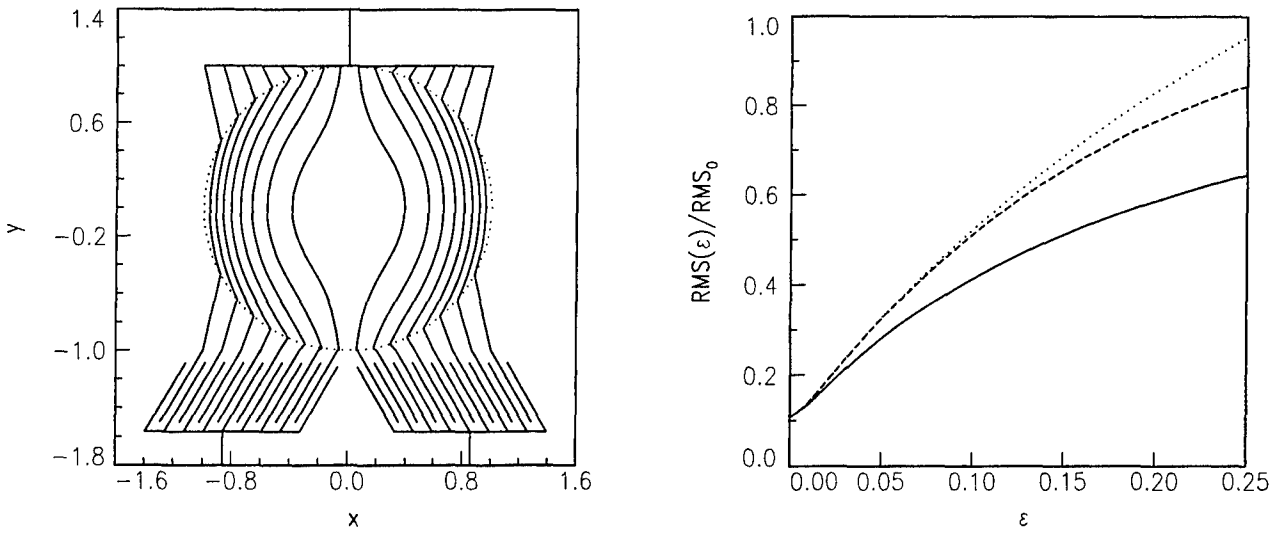

Figure 4. Left: Electrode segments for a Seidel coma cell with strip electrodes and resistor bench. The pupil rim is indicated with a dotted line. Right: The ratio of the RMS wavefront aberration to the original RMS_0 for the unbalanced case (dotted line), the balanced case (dashed line), and the asymmetric case (full line).

asymmetrically, so that $(V_+ + V_-)/2 \neq V_0$ (full line). Averaged over the ε range the performance is similar to that of the double Zernike cell, for small ε it is better, for large ε worse.

3. COVER LAYER THICKNESS COMPENSATION

3.1. Liquid Crystal Lens and Spherical Aberration

There are two ways to compensate for spherical aberration. The first one is to introduce spherical aberration into the light path with an LC-cell with segmented electrodes similar to the coma LC-cell discussed in the previous section or with an LC-cell with a non-segmented electrode and a ρ^4 thickness profile. The second way is to introduce defocus into the light path. The objective lens is designed to compensate for the spherical aberration arising from focusing through a cover layer. The compensation is ideal when the illuminating beam is collimated. In case the incident beam is slightly convergent or divergent the compensation is non-ideal and a net amount of spherical aberration is generated. It follows that cover layer thickness variations can be compensated by varying the vergence of the illuminating beam. This can be done with an LC-cell with a single non-segmented electrode and a spherical pit in one of the substrates. Fortunately, the tilt angle ψ of the LC director only depends on the applied voltage, and not on the varying cell-gap. This means that the voltage controls the refractive index independent of the surface profile, whereas the surface profile determines the type of aberrration. A spherical pit gives rise to a ρ^2 thickness profile, implying that defocus is generated by the LC-cell. When the curvature radius of the spherical pit R is large compared to the LC layer thickness in the middle of the pit d and to the thickness of the substrate glass plates the focal length of the LC-lens is:

$$f_{\mathrm{lc}} = \frac{R}{n_{\mathrm{lc}} - n_{\mathrm{g}}}, \tag{20}$$

with n_{lc} the refractive index of the LC, which is a function of the applied voltage, and with n_{g} the refractive index of the substrate glass.

3.2. Liquid Crystal Polymer Lens

An alternative type of LC-lens is made of photopolymerizable LC. Such a lens can be manufactured using more or less conventional LC-cell making, but without the transparant electrode layers. Instead of a conventional LC, a polymerizable LC in its monomer state is used. Alignment of the liquid crystal is possible because the monomer is a liquid. After cell making the LC is irradiated with UV-light, which initiates the formation of radicals that

start the polymerization reaction. The advantage of polymer LCs is the superfluousness of cell gap control. Also, it may be a birefringent lens that is easier and more cost-effective to manufacture than birefingent lenses made of conventional materials such as calcite.

Although such a type of lens is not continuously switchable it can be used for spherical aberration compensation by also using the ordinary polarization mode. For the extraordinary and ordinary modes we find focal lengths:

$$f_{\mathrm{e}} = \frac{R}{n_{\mathrm{e}} - n_{\mathrm{g}}}, \tag{21}$$

$$f_{\mathrm{o}} = \frac{R}{n_{\mathrm{o}} - n_{\mathrm{g}}}. \tag{22}$$

When the linear polarization can be rotated, for instance by a simple Twisted Nematic liquid crystal cell, the bifocal nature of the LC-lens can be used to compensate spherical aberration for two cover layer thickness values. This would be ideally suited for dual layer discs, i.e. discs that have two information layers at different depths.[3]

3.3. Aberrations of a Liquid Crystal Lens

It appears that LC-lenses suffer from astigmatism. This is due to the curvature of the pit region on one of the substrates, which causes a deformation of the liquid crystal director field, as drawn in Fig. 5. Due to the director tilt the refractive index of the extraordinary mode changes with x^2, whereas the spherical pit causes a thickness variation with $x^2 + y^2$. It follows that the lens must have astigmatism. A simple model can be used to estimate the amount of astigmatism. Consider a ray intersecting the lens at position (x, y). In the paraxial regime the ray is substantially parallel to the optical axis. Moreover, the lens thickness d is small compared to the curvature radius R. The optical path length for the ray traversing the pit is then given by:

$$\mathrm{OPL} = n_{\mathrm{g}} \frac{x^2 + y^2}{2R} + n_{\mathrm{lc}} \left[d - \frac{x^2 + y^2}{2R} \right]. \tag{23}$$

The liquid crystal director makes an angle $x/R \ll 1$ with the x-axis on the curved substrate side and is parallel to the x-axis on the non-curved side, giving an average director tilt angle $\psi = \pi/2 - x/2R$. The refractive index of the extraordinary mode is then approximately:

$$n_{\mathrm{lc}} = n_{\mathrm{e}} - \Delta n \left(\frac{x}{2R} \right)^2, \tag{24}$$

with the birefringence $\Delta n = n_{\mathrm{e}} - n_{\mathrm{o}}$. This expression follows from the general expression (1) when Δn is sufficiently small. This small birefringence approximation is usually quite justified in practice. It leads to an OPL:

$$\mathrm{OPL} = n_{\mathrm{e}} d - \frac{x^2}{2f_x} - \frac{y^2}{2f_y}, \tag{25}$$

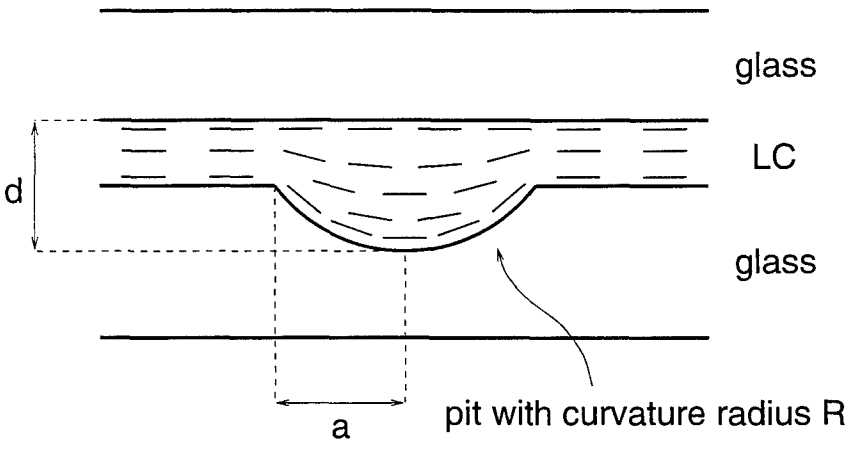

Figure 5. Deformation of the LC director field in the spherical pit, causing astigmatism. The drawing is not on scale.

where the x and y focal lengths are given by:

$$\frac{1}{f_x} = \frac{n_e - n_g}{R} + \frac{d\Delta n}{2R^2}, \tag{26}$$

$$\frac{1}{f_y} = \frac{n_e - n_g}{R}. \tag{27}$$

The lens is clearly astigmatic. The ratio of astigmatism to defocus is constant, and given by:

$$\frac{A_{22}}{A_{20}} = \frac{f_y - f_x}{f_y + f_x} = \frac{d\Delta n/R}{4(n_e - n_g) + d\Delta n/R}. \tag{28}$$

When the refractive index of the glass is matched to the ordinary refractive index of the LC ($n_g = n_o$), and using that $d \ll R$, we find the simple expression:

$$\frac{A_{22}}{A_{20}} = \frac{d}{4R}. \tag{29}$$

The defocus coefficient is $A_{20} = \Delta n a^2/4R$ with a the pupil radius. It then follows that the astigmatism coefficient is below the 1 mλ level if $d\Delta n(a/R)^2/16\lambda$ is smaller than 1×10^{-3}. In practice Δn is approximately 0.10 leading to the criterion for sub-mλ astigmatism:

$$\frac{a}{R} \leq 0.4\sqrt{\frac{\lambda}{d}}. \tag{30}$$

Clearly, a large radius of curvature (small NA) and/or a small thickness are advantageous from the point of view of aberrations.

The results may be generalized to the case with a director tilt due to the rubbing treatment or to an applied voltage. Defining ψ as the effective director tilt angle the LC refractive index is:

$$n_{lc} = n_e - \Delta n \sin^2\left(\pi/2 - \psi + \frac{x}{2R}\right) = n_e - \Delta n \cos^2\psi - \Delta n \sin(2\psi)\frac{x}{2R} + \Delta n \cos(2\psi)\left(\frac{x}{2R}\right)^2 + \ldots. \tag{31}$$

Clearly, the effective birefringence is reduced to $-\Delta n \cos(2\psi)$ and a wavefront tilt proportional to $\Delta n \sin(2\psi)$ is introduced. The resulting astigmatism is:

$$\frac{A_{22}}{A_{20}} = \frac{-d\Delta n \cos(2\psi)}{4R(n_e - \Delta n \cos^2\psi - n_g)}. \tag{32}$$

Finally, it is mentioned that the case with two curved surfaces (with radii R_1 and R_2) can be described by replacing $1/R$ by $1/R_1 - 1/R_2$ in all previously derived formulas.

Astigmatism of birefringent lenses is first considered by Kikuta et. al..[4] They considered the case of a lens with a uniform uniaxial symmetry axis and found that there is astigmatism provided that both surfaces of the lens are curved. In the present case, the astigmatism is rooted in the liquid crystalline nature of the birefringent lens, causing a deformation of the uniaxial symmetry axis that is ultimateley responsible for the aberration. As opposed to the Kikuta type of astigmatism lenses with possibly one flat surface also suffer from astigmatism.

3.4. Experiment

Laboratory samples of polymer LC-lenses have been made by making a spherical pit with curvature radius of 100 mm in a flat 3 mm thick plate of glass. With a pit diameter of 3.5 mm, the depth of the pit in the centre is 15 μ. The overall thickness of the LC-layer was approximately 50 μ. For 632.8 nm light the resulting astigmatism is approximately 0.4 mλ, i.e. negligible. The other substrate was a flat, 1 mm thick plate of glass. Polyimide alignment layers were applied on both substrates by spincoating, and subsequently cured and rubbed in order to induce alignment of the LC molecules. Both substrates were squeezed together with a droplet of LC in between them. The LC-mixture was composed of 50% E7-diacrylate, 49% E7, and 1% photo-initiator. Domains in the LC alignment were eliminated by heating the LC above the clearing point and subsequently cooling down to room temperature. Finally, the mixture was polymerized using UV-light. The uniformity of the LC alignment was checked by polarization microscopy. The quality of the polymer LC lenses were measured for 632.8 nm laser light

polarized by a sheet polarizer with a shearing interferometer.[5] Focal lengths $f_e = 0.54$ m and $f_o = 12.4$ m (n_o and n_g are nearly matched) were obtained. The measured pupil was reduced to 90% of the pit diameter, i.e. the pupil diameter was 3.15 mm, leading to numerical apertures $NA_e = 2.9 \times 10^{-3}$ and $NA_o = 1.3 \times 10^{-4}$. Despite the small NA values aberration levels of RMS_e=37 mλ, and RMS_o=13 mλ (relative to the region surrounding the pit) were measured, mainly consisting of astigmatism. This is probably due to the assembly of the two glass plates, which turned out to be not sufficiently parallel for the measured sample. Improvement of the assembly may reduce the aberrations to a negligible level.

4. SUMMARY AND CONCLUSION

Liquid crystals can be applied in aberration compensation devices. Such devices can be quite beneficial for high NA optical recording formats.

The sensitivity to disc tilt can be decreased by a coma generating LC-cell. However, astigmatism is generated when the objective lens is decentered w.r.t this compensating LC-cell. Several solutions for this problem are discussed; attaching the compensator to the actuator, balancing the compensated coma and the generated astigmatism, using mutually displaced segmented electrodes on both sides of the cell, and correcting for Seidel coma instead of Zernike coma.

Liquid crystal lenses can be used to illuminate the objective lens with variable vergence thereby generating spherical aberration. This can be used to correct for cover layer thickness variations. A birefringent lens made of polymer LC is a viable alternative for lenses made of conventional birefringent materials such as calcite. The LC is aligned in its monomer state and subsequently cured by UV-irradiation. It appears that LC polymer lenses are always astigmatic. However, when the thickness and/or the NA of the lens is sufficiently small this aberration is negligible.

ACKNOWLEDGMENTS

Peter van de Witte, Joost Vogels, and Cor Adema are credited for their help in preparing polymer LC lenses.

REFERENCES

1. T. Narahara, S. Kobayashi, M. Hattori, Y. Shimpuku, G. van den Enden, J. Kahlman, M. van Dijk, and R. van Woudenberg, "Optical disc system for digital video recording," *Joint International Symposium on Optical Memory and Optical Data Storage, SPIE Vol.* **3864**, pp. 50–52, 1999.
2. N. Murao, M. Iwasaki, and S. Ohtaki, "Tilt servo using a liquid crystal device," *International Symposium on Optical Memory* , pp. 351–353, 1996.
3. K. Kurokawa, M. Naito, K. Yasuda, T. Kashiwagi, and O. Kawakubo, "A 16.8 GB double-decker phase change disc," *Joint International Symposium on Optical Memory and Optical Data Storage, SPIE Vol.* **3864**, pp. 197–199, 1999.
4. H. Kikuta, K. Iwata, and H. Shimomura, "First-order aberration of a double-focus lens made of a uniaxial crystal," *J. Opt. Soc. Am. A* **9**, pp. 814–819, 1992.
5. M. Mantravadi, "Lateral shearing interferometry," in *Optical Shop Testing*, D. Malacara, ed., pp. 123–172, John Wiley & Sons, New York, 1992.